

Tunable high-harmonic generation by chromatic focusing of few-cycle laser pulses

W. Holgado,^{1,*} C. Hernández-García,¹ B. Alonso,^{1,2} M. Miranda,³ F. Silva,^{2,4}
O. Varela,⁵ J. Hernández-Toro,⁵ L. Plaja,¹ H. Crespo,^{2,1} and I. J. Sola^{1,†}

¹*Grupo de Investigación en Aplicaciones del Láser y Fotónica,
Departamento de Física Aplicada, Universidad de Salamanca, E-37008 Salamanca, Spain*

²*IFIMUP-IN and Departamento de Física e Astronomia,
Universidade do Porto, Rua do Campo Alegre 687, 4169-007 Porto, Portugal*

³*Department of Physics, Lund University, P.O. Box 118, SE-221 00 Lund, Sweden*

⁴*Sphere Ultrafast Photonics, Lda, R. Campo Alegre 1021, Edifício FC6, 4169-007 Porto, Portugal*

⁵*Centro de Láseres Pulsados, CLPU, Villamayor de la Armuña, C/ Adaja 8, E-37185, Spain*

(Dated: December 3, 2024)

In this work we study the impact of chromatic focusing of few-cycle laser pulses on high-order harmonic generation (HHG) through analysis of the emitted extreme ultraviolet (XUV) radiation. Chromatic focusing is usually avoided in the few-cycle regime, as the pulse spatio-temporal structure may be highly distorted. Here, however, we demonstrate it as an additional control parameter to modify the generated XUV radiation. We present experiments where few-cycle pulses are focused by a singlet lens in a Kr gas jet. The chromatic distribution of focal lengths allows us to tune HHG spectra by changing the relative singlet-target distance. Interestingly, we also show that the degree of chromatic aberration needed to this control does not degrade substantially the harmonic conversion efficiency, still allowing for the generation of supercontinua with the chirped-pulse scheme, demonstrated previously for achromatic focussing. We back up our experiments with theoretical simulations reproducing the experimental HHG results depending on diverse parameters (input pulse spectral phase, pulse duration, focus position) and proving that, under the considered parameters, the attosecond pulse train remains very similar to the achromatic case.

INTRODUCTION

Few-cycle pulses are of great interest for attosecond science, allowing the generation of isolated attosecond pulses via high-harmonic generation (HHG) [1, 2], atomic and molecular dynamic studies [3], ultrafast spectroscopy (e.g., transient absorption [4]) and spectral interference in the extreme ultraviolet (XUV) range [5], among others. Nowadays, intense few-cycle pulses in the near-visible to infrared (IR) domain are available thanks to the development of ultrashort pulse lasers combined with post-compression techniques (e.g., based on gas-filled hollow-core fibers (HCF) [6, 7] or filamentation in gases [8]). Proper output spectral phase compensation may directly lead to sub-1.5 cycles pulse compression [9], and special setups allow to synthesize even sub-cycle pulses [10].

Apart from the complexity of their generation, few-cycle pulses are extremely sensitive to dispersion in the propagation medium and are also prone to spatio-temporal distortions. Thus, in order to preserve the duration and spatio-temporal properties of few-cycle pulses, focusing with achromatic and non-dispersive systems, such as spherical mirrors or off-axis parabolic reflectors [11], is required. However, few-cycle pulses obtained by post-compression techniques typically exhibit spatio-temporal structure. In the case of filamentation this is more evident [12], but spatial dependence is also present when using the gas-filled HCF technique, namely in the form of spatial chirp [13]. Incidentally, controlling the spatio-temporal structure of the beam may be used to exert additional control over nonlinear light-matter in-

teraction processes. Using diffractive optical elements (DOEs) [14] or lenses exhibiting some aberrations, is a simple way to introduce a spatio-temporal structure in ultrashort laser pulses. For instance, chromatic focal aberrations allow to tune the second harmonic wavelength by simply adjusting the distance between the nonlinear crystal and the focusing element [15]. Also, chromatic focusing can be used to tune the broad spectrum resulting after a filamentation process [16]. In addition, including astigmatic focusing allows for the generation of more stable, spectrally broader, higher energy filaments [17] than for the non-astigmatic case. Aberrated focusing is also used to improve the axial resolution and to extend the penetration depth in nonlinear confocal microscopy [18].

The control of HHG through the introduction of aberrations to the fundamental beam would have practical implications in fields such as XUV spectroscopy or the temporal shaping of attosecond pulses. In fact, pulse front tilt has already been proven as a useful tool to generate angle-dependent XUV radiation emission [19], allowing one to spatially filter isolated attosecond bursts. Similarly, angular chirping of the driving field can be used to generate XUV radiation with controlled angular distribution of the spectra [20]. Therefore, what is an *a priori* detrimental aberration can be turned into a useful tool.

In this work we explore experimentally and theoretically high-order harmonic generation driven by few-cycle pulses chromatically focused with a normal-dispersion convergent singlet lens. Chromatic aberration affects the driving IR light distribution at the focal region as: focal length is shorter (longer) for shorter (longer) wave-

lengths. As a result, we introduce a new degree of control of the XUV spectrum characteristics. In particular, we demonstrate that it is possible to shift the XUV spectrum and to modify the spectral content while maintaining the yield and attosecond train structure similar to the obtained with achromatic focusing. The experiments are complemented and corroborated by numerical simulations of the focusing scheme in a macroscopic gas sample. This paper is organized as follows: first, the experimental and theoretical procedures are described; second, the experimental results are shown; then, the theoretical results are presented, discussing the role of the chromatic focusing as a new control parameter of the HHG process.

EXPERIMENTAL AND THEORETICAL METHODS

For the experiments we used a 1-kHz Ti:Sapphire CPA amplifier (Femtolasers Produktions FemtoPower Compact Pro CEP) delivering pulses with a Fourier-transform limit duration of 25 fs of full-width at half-maximum (FWHM). The output pulse is post-compressed in a HCF with an inner diameter of 250 micrometers and 1-meter length. The HCF was filled with Argon at 1 bar. By compensating the spectral phase with 10 bounces off chirped mirrors (Ultrafast Innovations; nominal GDD: -20 fs^2 per bounce at 800 nm, minimum reflectance: 99%), 5-fs (and shorter) pulses with an energy up to 300 μJ are routinely obtained [9, 13]. Pulse duration can be tuned by changing the post-compression gas pressure and re-adjusting the spectral phase compensation. In the present work, pulse duration covered the range between 3.3 fs and 8.0 fs.

The laser pulse was then focused into a krypton gas jet by a BK7 glass singlet lens ($f = 30 \text{ cm}$ at $\lambda = 800 \text{ nm}$), which provided the desired chromatic focusing scheme. We also performed experiments with an achromatic focusing scheme for comparison. For the latter we employed a spherical silver mirror ($f = 50 \text{ cm}$). Both the lens and the spherical mirror were placed on a translation stage, so the focus position could be controlled and scanned. The pulse entered the vacuum chamber through a 0.5 mm thick fused-silica window, which was placed close to the focusing element to avoid any potential nonlinear effects. HHG was performed in a krypton gas jet (5 bar of backing pressure), with a nozzle of 500 μm diameter. The pressure inside the vacuum chamber where the high-order harmonics were generated was around 5×10^{-3} mbar. A 150-nm thick aluminum foil was used to filter out the IR radiation and the lower-order harmonics, while the higher orders (with energies between 17 eV and 70 eV) can propagate through it. The XUV spectra were characterized with a grazing-incidence Rowland circle XUV spectrometer (Model 248/310G, McPherson Inc.), of 1-m radius, equipped with a 300 grooves/mm

spherical diffraction grating. The carrier-envelope phase (CEP) of the seed oscillator (Femtolasers Produktions Rainbow CEP) was stabilized with a fast loop and its stability was not significantly altered by the subsequent amplification and post-compression processes, which resulted in an rms of approximately 100 mrad throughout each measurement without the need to employ a slow loop [21]. The driving few-cycle laser pulses were characterized using the d-scan technique [9, 22], which can measure pulses down to single-cycle durations [9, 23].

We performed numerical simulations of HHG including both microscopic (single-atom) and macroscopic (phase-matching) physics. The dipole acceleration of each elementary emitter was calculated using an extension of the strong field approximation [24] (due to the lack of simple analytical expressions for the matrix elements of the acceleration in krypton, we have performed our calculations in argon, that has the same parity for the valence electron and a similar ionization potential), while harmonic propagation and the collective response were worked out using a method based on the electromagnetic field propagator [25]. The gas jet was modelled with a Gaussian density distribution along the laser propagation direction with a width of 1-mm (FWHM) and a peak pressure of 10 mbar. The signal at the far field detector was computed as the coherent addition of the HHG contributions of all the elementary sources, where the HHG light was assumed to propagate to the detector with a phase velocity c . In this process, phenomena such as time-dependent group velocity walk-off [26], absorption of the harmonics, plasma and neutral dispersion were all taken into account. At the pressures used in this work, nonlinear phenomena in the propagation of the driving IR beam were negligible. This model has been tested on several scenarios where phase matching in a gas jet is a relevant factor in HHG [21, 27–31]. In this work, and in order to simulate experiments where the driving beam was focused with a singlet lens, the chromatic effect was also taken into account, using the Sellmeier coefficients for the lens material, when calculating the laser field within the gas region.

EXPERIMENTAL RESULTS

When focusing broadband pulses with a system exhibiting chromatic aberration, the focal length depends on the wavelength. Thus, if such a beam is used for driving a nonlinear process, as HHG, the spectrum of the generated radiation will strongly depend on the relative position of the medium with respect to the nominal beam focus. In this situation, the XUV spectra will be modified by the lens position in coordinate z .

To confirm the latter point, we measured the harmonic spectra varying the distance (z coordinate) between the focusing element and the gas jet (we shall refer to this as HHG z -scan, not to be confused with the nonlinear

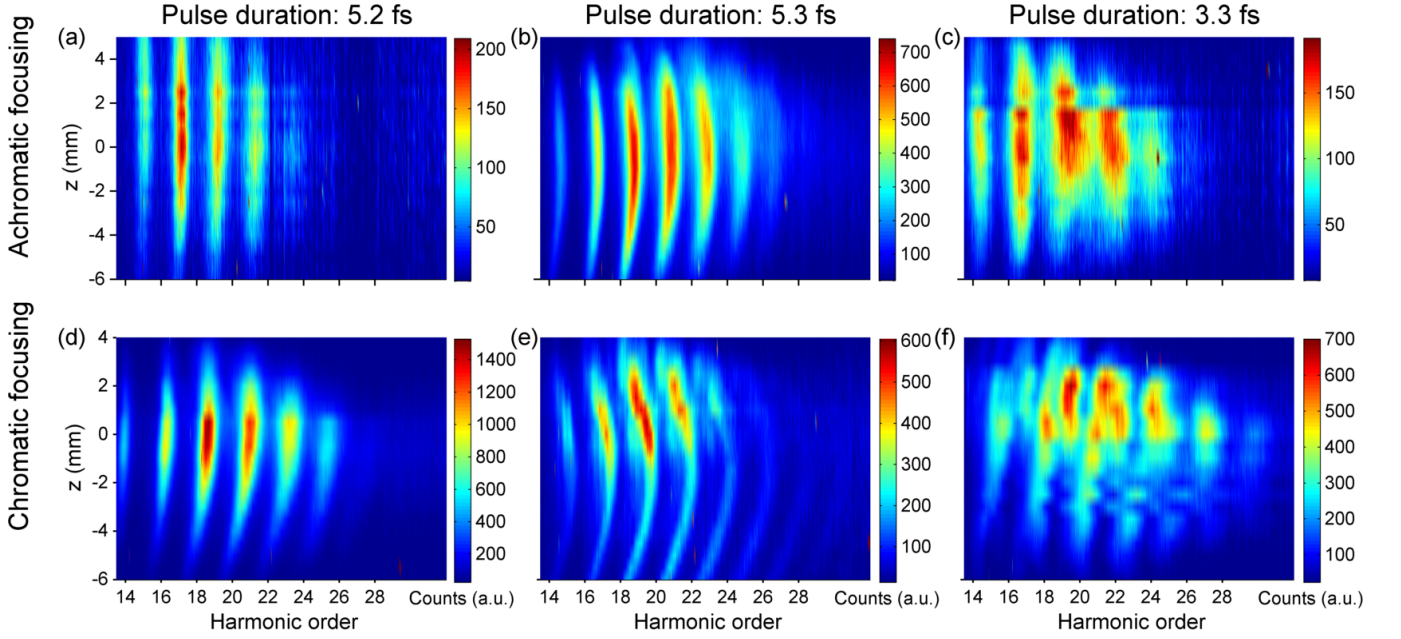


FIG. 1. **HHG z -scans for chromatic and achromatic case:** HHG on Kr depending on focusing system-target distance z ($z = 0$ mm stands for focus on gas jet, $z < 0$ for focus before gas jet, $z > 0$ for focus after gas jet) for three different driving pulses (shown in Fig. 2): (a, d) 5.2 fs FWHM pulse (Fourier limit: 3.35 fs) with residual third order dispersion, (b, e) 5.3 fs FWHM pulse (Fourier limit: 4.9 fs) and (c, f) 3.3 fs FWHM pulse (Fourier limit: 2.9 fs). First row figures (a-c) correspond to focusing with a silver spherical mirror ($f = 50$ cm), and the lower row (d-f) to focusing with a BK7 singlet ($f = 30$ cm).

material characterization technique called z -scan). The $z = 0$ position here stands for focus on gas jet, $z < 0$ for focus before gas jet and $z > 0$ for focus after gas jet. Fig. 1 shows a set of HHG z -scans ranging different input pulse conditions (5.2 fs FWHM pulses, exhibiting strong third order dispersion, TOD, for figures 1a and 1d; 5.3 fs FWHM pulses, with compensated TOD for figures 1b and 1e and 3.3 fs FWHM pulses for figures 1c and 1d) and focusing schemes (upper row corresponds to the case focusing with the spherical mirror and lower row stands for singlet lens focusing). The input pulse reconstructions corresponding to the considered cases are shown in Fig. 2.

Fig. 1a confirms that, when a spherical mirror is used, the spectral position of the harmonics remains unaltered when the distance between the focusing mirror and the gas jet is change. This can be understood since no chromatic aberration is present. In this case, the 5.3 fs FWHM input pulse exhibits residual TOD (see Fig. 2a and 2b), what is very common after post-compression process and it is caused by the nonlinear process inside the hollow-core fiber under optimized propagation conditions [32], being previously observed in several works [9, 17, 33–35].

For studying the impact of the residual TOD, we adjusted the driving pulse post-compression to decrease the TOD contribution, while maintaining a similar pulse duration, 5.3 fs FWHM (Fig. 2c and 2d). Then, the HHG z -scan varies from the previous, z -coordinate independent

case, since some spectral broadening, in particular at higher harmonics, is observed at $z > 0$ focusing positions (Fig. 1b). This spectral broadening, as recently reported in Ref. [21] at the same pulse duration regime, results from a joint effect at the atomic (HHG is altered by particular input pulse spectral phases) and the macroscopic levels (due to collective coherent addition, phase matching fills the harmonic spectrum, enhancing the continuum structure and smoothing out spectral peaks). Furthermore, Fig. 1c shows that the spectral broadening at $z > 0$ focusing position is increased when using shorter pulses (3.3 fs FWHM, whose reconstruction are shown in Fig. 2e and 2f). Please note that for $z < 0$, where the spectral broadening does not manifest, the XUV spectrum position remain insensitive to the z coordinate, as should be expected from an achromatic focusing scheme.

In order to analyze the chromatic focusing effect, Fig. 1 lower row presents the corresponding HHG z -scan measured while focusing with the singlet. Fig. 1d reveals that the chromatic focusing scheme introduces a dependence of the harmonic position on z , in contrast with was observed using achromatic focusing (Fig. 1a) and the same input pulse characteristics. In fact, it follows the first intuitive guess: when moving the lens in order to place the nominal focus after (before) the gas jet, i.e. $z > 0$ ($z < 0$), a blue shift (red shift) of the harmonic spectrum should be observed. Since no additional effect alter the XUV spectra, this dependence is observed clearly. However, the presence of the above commented spectral

broadening phenomenon is able to alter this neat behavior under other experimental conditions. As shown in Fig. 1e, for $z > 0$, XUV spectra becomes broader and its dependence on z is the opposite as expected from pure chromatic effect. Nevertheless, when the broadening spectrum effect is not present, i.e. at $z < 0$, the spectral shift induced by the chromatic focusing prevails, shifting the harmonic spectral positions away from the measured in its corresponding achromatic focusing case (Fig. 1b). This occurs similarly when shorter input pulses, 3.3 fs FWHM, are used, since at $z > 0$ spectral broadening is present, even enhanced (e.g., continuous spectra arise), but for $z < 0$ the spectral shift matches with the expected from the used chromatic focusing, in contrast also with the observed z insensitivity observed in the achromatic case (Fig. 1c). Thus, chromatic focusing effectively allows one to vary the HHG spectrum and to tune it by just moving the lens position.

The HHG z -scan in the few-cycle pulse regime is extremely sensitive to experimental conditions. As an example, Fig. 3 shows the z -scan harmonic intensity profile for several CEPs of the driving pulse (pulse energy of 56 μ J, pulse duration: 3.6 fs FWHM, Fourier limit: 2.9 fs FWHM). In this regime, due to the chromatic focusing,

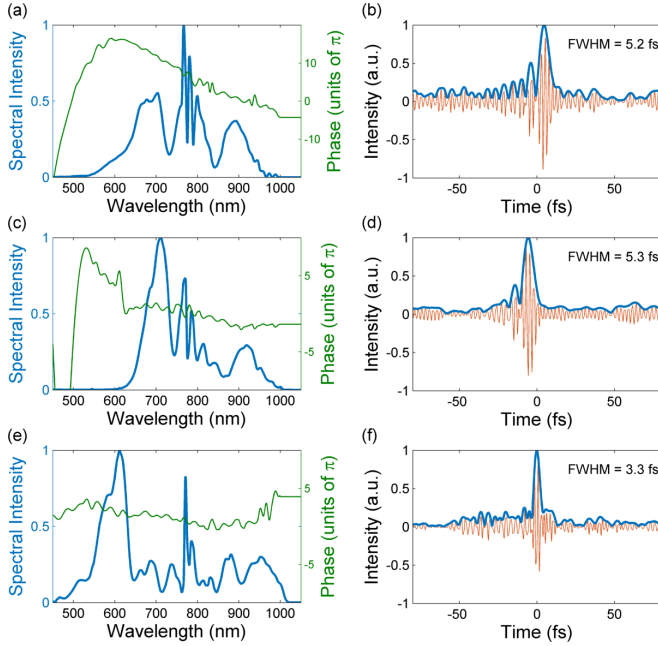


FIG. 2. **Characterization of the driving pulses:** Left column: Spectra (blue line) and spectral phase (green line); right column: time dependent electric field amplitude (blue line) of the three pulses used for the HHG z -scan shown in Fig. 1. Upper row shows a pulse with higher dispersion order, and corresponds to Fig. 1(a) and (d). Second row displays a pulse closer to its Fourier limit duration, where the spectral phase is flatter than in the previous case, and corresponds to Fig. 1(b) and (e). Lower row presents a shorter pulse, lasting less than 1.5 cycles, which corresponds to Fig. 1(c) and (f).

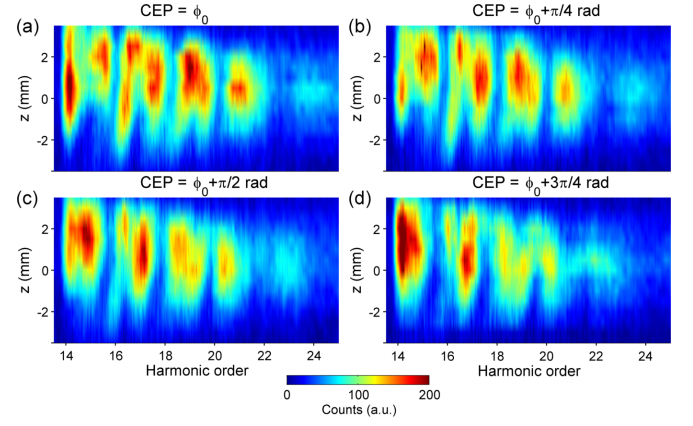


FIG. 3. **CEP-dependence of the chromatic HHG z -scan:** HHG z -scan using Kr (backing pressure of 6 bar) as a function of singlet-target distance in the few-cycle pulse regime (pulse energy of 56 μ J, time duration: 3.6 fs FWHM, Fourier limit: 2.9 fs FWHM) for different values of CEP: (a) ϕ_0 , (b) $\phi_0 + \pi/4$, (c) $\phi_0 + \pi/2$, (d) $\phi_0 + 3\pi/4$.

pulse structure (even at the level of the electric field oscillation) has great relevance, and phase changes in the electric field of the pulses directly affect the HHG z -scan.

In order to study the effects of chromatic focusing in the XUV continuum generation, we have performed a dispersion-scan for the different studied cases. The coordinate z (i.e. position of the lens) has been chosen to optimize the spectral broadening. A dispersion-scan was performed by adding or extracting material on the light path prior to the focusing element. In our case, we used a pair of BK7 wedges (with an angle of 8°). The insertion of dispersive material in the optical path was changed by laterally moving one of the BK7 wedges. In the case of the 5.3 fs FWHM pulse (Fig. 2d) used for Fig. 1e, the z coordinate was fixed at $z = 1$ mm and a dispersion-scan was performed (Fig. 4a). The scan shows a behavior very similar to that observed when focusing the same pulse achromatically (with the spherical mirror of $f = 50$ cm), as shown in Fig. 2b in [21]. For positive chirp the HHG spectra feature narrow peaks at odds harmonics, while for negative chirp, spectral broadening is observed. The observed high frequency fringes denote the CEP dependence of the HHG (i.e. in a short range of BK7 length variation the dispersion-scan becomes a CEP scan). This behavior of the XUV radiation has been observed previously in other works using achromatic focusing [36, 37].

When shorter pulses (e.g., 4 fs) are used (Fig. 4b) the spectrum changes depending on the dispersion are more pronounced, from well-defined harmonics at positive chirp to spectral broadening at negative chirp, until eventually becoming continua, ranging over 8 harmonic orders in this case, resembling the dependence reported case for achromatic focusing ([21]). This suggests that the continuum mechanism remains the same as de-

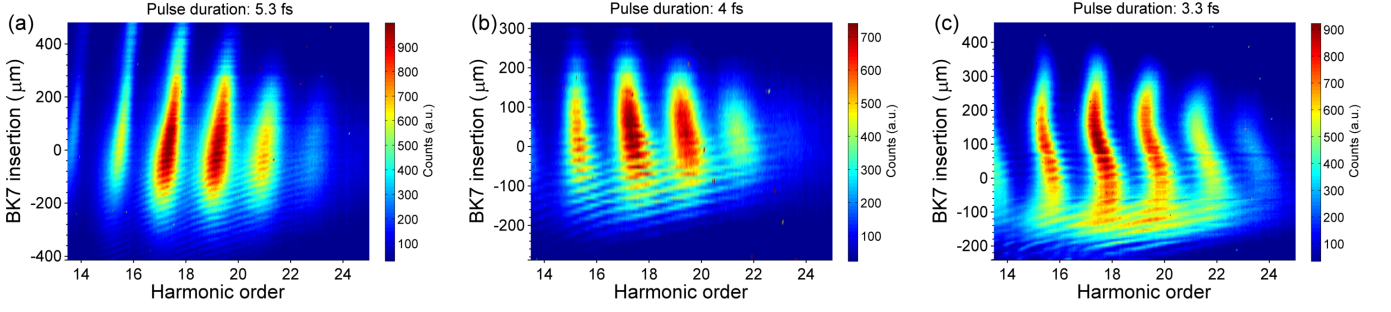


FIG. 4. **HHG dispersion-scans with chromatic focusing:** HHG performed in krypton in three different cases: (a) Pulse duration of 5.3 fs and energy of 80 μJ , (b) duration of 4 fs and 50 μJ , (c) duration of 3.3 fs and 50 μJ . Focus is placed 2 mm after the gas jet in (a) and (b), while it is placed at the gas jet position in (c). Pulse durations are measured at 0 μm of BK7 insertion.

scribed for achromatic focusing at this pulse duration range. However, shorter pulses in the few-cycle regime reveal differences in the dispersion-scan. Fig. 4c features a dispersion-scan for a 3.3 fs pulse (Fig. 2f), where the z coordinate was fixed at $z = 0$ mm (the corresponding z -scan is depicted in Fig. 1f). In this case, the continuum spans over 12 harmonic orders and, in contrast with the precedent examples, the harmonic yield of continuum spectrum is higher than the one obtained at the same scan in other chirp conditions. Thus, a controlled and limited chromatic focusing does not alter the ability to generate spectral continua through fundamental pulse chirp and phase matching variations.

THEORETICAL RESULTS AND DISCUSSION

Aiming to understand the role of the singlet lens in more detail, we studied the effect of chromatic focusing on the HHG, i.e., how chromatic aberration affects the harmonic emission at the microscopic (single-atom) and macroscopic (phase-matching) levels. Numerical simulations have been performed by scanning the pulse duration and lens-gas distance. Because of the relatively long computational time of HHG dispersion-scan simulations, and the extensive range of the scanned parameter space when analyzing the effects of chromatic focusing, we assumed Fourier-limited input pulses (at 0 μm BK7 material insertion in the dispersion-scans).

Fig. 5 shows the HHG spectra corresponding to the dispersion-scan of a 4.8 fs FWHM pulse at Fourier limited conditions, focused by a $f = 30$ cm singlet and with the nominal focus placed 2 mm after the gas jet (i.e., $z = 2$ mm). We show the results from the single atom response (microscopic, Fig. 5a) and including propagation (macroscopic, Fig. 5b).

When comparing the chromatic and achromatic cases, while the dispersion-scans for single atom response (Fig. 5a compared with Fig. 3a of [21]) present some differences between the two focusing schemes, the correspond-

ing macroscopic response (Fig. 5b versus Fig. 3b of [21]) are very similar in their general structure and yield. The chromatic focusing case shows a slight blue shift in the generated harmonics, due to chromatic aberration. Surprisingly, phase matching when focusing with the singlet and its associated chromatic aberration can perform slightly better than aberrationless focusing. In addition, theoretical simulations (Fig. 5b) show a good qualitative matching with experimental results (Fig. 4a). According to simulations, the structure of the XUV continuum is the same than the one obtained for spherical mirror focusing [21]: three main attosecond pulses with relative phase differences that yield via spectral interference (Fig. 6). Therefore, no major attosecond pulse time structure distortions would be produced by the considered chromatic aberration referred to the achromatic focusing case.

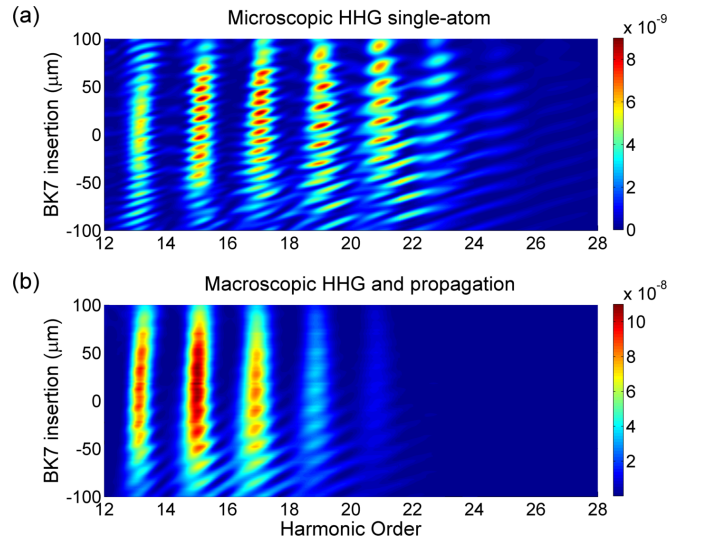


FIG. 5. **Numerical simulation of HHG with chromatic focusing:** Dispersion-scan of far field on-axis HHG for Fourier limited pulse of 4.8 fs FWHM focused with a $f = 30$ cm singlet lens. Single atom response is depicted in (a) and collective response including propagation effects in (b).

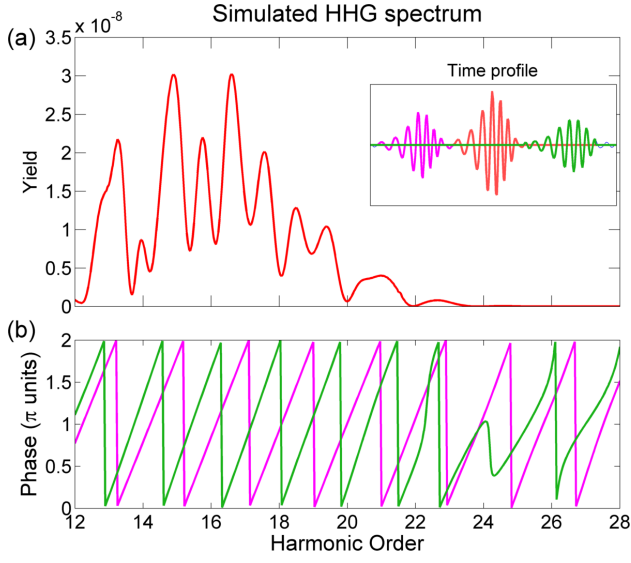


FIG. 6. **HHG driven by negatively chirped pulse:** Simulated on-axis far-field XUV collective response spectra when 92 μm of BK7 have been removed from the Fourier-limit condition (4.3 fs pulse duration at the Fourier limit), focusing with a $f = 30$ cm singlet. The corresponding time evolution is shown in the inset for propagated calculations, denoting at different colors the main individual attosecond pulses. (b) Corresponding spectral phase differences between the first and second attosecond pulses (violet line) and between the second and third pulses (green line) for propagated calculations.

In order to gain further insight on the HHG response to the dispersion-scans in the few-cycle pulse regime, we also performed simulations with shorter pulses (2.9 fs FWHM, on the order of durations currently experimentally available [23]). In Fig. 7 we show the results obtained when focusing with the singlet with its nominal focus 2 mm before (Fig. 7a, $z = -2$ mm) and after (Fig. 7b, $z = 2$ mm) the gas jet. In the former case, phase-matching is responsible for the suppression of the middle plateau, while in the latter a continuum arises for chirped pulses. Note that the harmonics in Fig. 7a are red-shifted in relation to Fig. 7b because of the chromatic aberration.

When comparing chromatic (Fig. 7b) and achromatic focusing (Fig. 7c), the general structure is similar, and the maximum harmonic yield is the same. Hence, theoretically chromatic focusing can generate harmonics as efficiently as achromatic focusing. When comparing experiment (Fig. 4) and simulations (Fig. 7) for the chromatic case, the dispersion-scan presents similarities for negatively chirped pulses: appearance of a continuum and peak shifted when the CEP is varied. However, the behavior for positive chirp differs, possibly due to the fact that simulations consider a Fourier limited input pulse, while the experimental pulse presented some high order spectral phase components (TOD and higher, as it can be deduced from spectral phase reconstruction of the in-

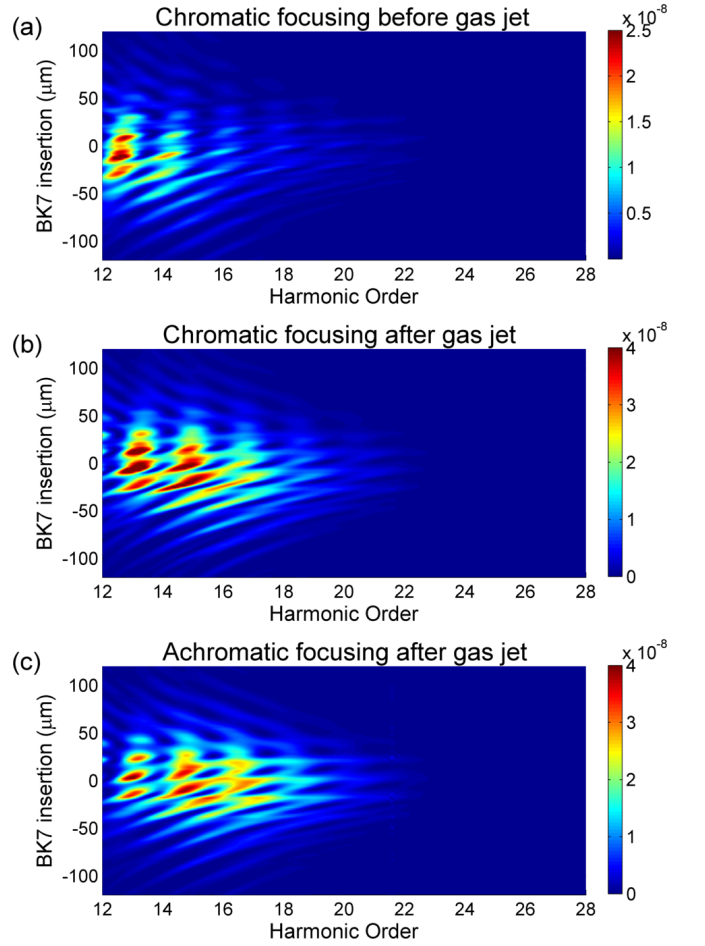


FIG. 7. **HHG comparison for chromatic and achromatic focusing:** Dispersion-scan of far field on axis HHG for a 2.9 fs pulse (Fourier limit) focusing with a $f = 30$ cm singlet at 2 mm before the gas jet (a), 2 mm after the gas jet (b) and with a spherical mirror ($f = 40$ cm) at 2 mm after the gas jet (c).

put pulse, shown in Fig. 2e) that are known to affect the dispersion-scans [9]. In fact, harmonic spectral shifts along dispersion-scans (e.g., as seen in Fig. 4), suggest the presence of higher order phase contribution in the experiments, while no such shift appears in the theoretical dispersion-scans for pulses free of high-order spectral phase components (Fig. 5 and Fig. 7).

CONCLUSIONS

To conclude, contrary to what is commonly expected, focusing ultra-broadband pulses with some chromatic dependence (e.g., with a singlet lens) can provide a useful degree of control of the resulting HHG process, yielding interesting and potentially useful spectral effects. The focusing of each wavelength component at different focal lengths has an impact in the single atom emission

across the generating region and also in the coherent addition of the XUV light from all the elemental emitters. Therefore, an additional experimental parameter, the chromatic focal distribution, can be used for altering the XUV characteristics. To show it, we have used a singlet with broadband few-cycle pulses, introducing chromatic aberration. We have observed that it is possible to tune the harmonics by changing the singlet position when focusing few-cycle pulses, since the spectral content of the focus changes because of the chromatic aberration. This ability can be useful to perform spectroscopy in the XUV region. On the other hand, the employed focusing scheme does not change some of the properties observed in HHG using achromatic focusing, namely generation of spectral XUV continua even in the low-order harmonic region under adequate pulse (here shown from 20 eV to 39 eV) and phase matching conditions. Furthermore, it produces XUV radiation with a similar yield.

Full propagation theoretical simulations confirm that the chromatic focusing reproduces the temporal structure obtained in the achromatic case. Finally, since the HHG process is distributed in different spacial regions depending on the wavelengths, further control over the chromatic focusing (e.g. using diffractive lenses, adaptive optics, etc.) and the gas distribution profile may allow to tailor the phase matching conditions with an additional control parameter offering further optimization of the HHG process.

ACKNOWLEDGMENTS

We acknowledge support from Junta de Castilla y León (Projects No. SA116U13 and SA046U16), Spanish MINECO (Grants No. FIS2009-09522, No. FIS2013-44174 P, No. FIS2015-71933-REDT and No. FIS2016-75652-P). This work was partly supported by Fundação para a Ciência e Tecnologia, Portugal, co-funded by COMPETE and FEDER, via Grants PTDC/FIS/122511/2010 and UID/NAN/50024/2013; F.S. acknowledges support from Grant SFRH/BD/69913/2010 and B.A. acknowledges support from Post-Doctoral Fellowship SFRH/BPD/88424/2012; H.C. acknowledges support from Sabbatical Leave Grant SFRH/BSAB/105974/2015. C.H-G acknowledges support from a Marie Curie International Outgoing Fellowship within the EU Seventh Framework Programme for Research and Technological Development, under REA Grant Agreement No. 328334.

* warein@usal.es; Present Address: Centro de Láseres Pulsados, CLPU, Villamayor de la Armuña, C/ Adaja 8, E-37185, Spain

† ijsola@usal.es

- [1] M. Hentschel, R. Kienberger, C. Spielmann, G. A. Reider, N. Milosevic, T. Brabec, P. B. Corkum, U. Heinzmann, M. Drescher, and F. Krausz, *Nature* **414**, 509 (2001).
- [2] G. Sansone, E. Benedetti, F. Calegari, C. Vozzi, L. Avaldi, R. Flammini, L. Poletto, P. Villoresi, C. Altucci, R. Velotta, S. Stagira, S. D. Silvestri, and M. Nisoli, *Science* **314**, 443 (2006).
- [3] P. B. Corkum and F. Krausz, *Nat. Phys.* **3**, 381 (2007).
- [4] E. Goulielmakis, Z.-H. Loh, A. Wirth, R. Santra, N. Rohringer, V. S. Yakovlev, S. Zherebtsov, T. Pfeifer, A. M. Azzeer, M. F. Kling, S. R. Leone, and F. Krausz, *Nature* **466**, 739 (2010).
- [5] S. Fuchs, A. Blinne, C. Rödel, U. Zastrau, V. Hilbert, M. Wünsche, J. Bierbach, E. Frumker, E. Förster, and G. G. Paulus, *Appl. Phys. B* **106**, 789 (2012).
- [6] M. Nisoli, S. De Silvestri, and O. Svelto, *Appl. Phys. Lett.* **68**, 2793 (1996).
- [7] S. Sartania, Z. Cheng, M. Lenzner, G. Tempea, C. Spielmann, F. Krausz, and K. Ferencz, *Opt. Lett.* **22**, 1562 (1997).
- [8] C. Hauri, W. Kornelis, F. Helbing, A. Heinrich, A. Couairon, A. Mysyrowicz, J. Biegert, and U. Keller, *Appl. Phys. B* **79**, 673 (2004).
- [9] F. Silva, M. Miranda, B. Alonso, J. Rauschenberger, V. Pervak, and H. Crespo, *Opt. Express* **22**, 10181 (2014).
- [10] A. Wirth, M. T. Hassan, I. Grguraš, J. Gagnon, A. Moulet, T. T. Luu, S. Pabst, R. Santra, Z. Alahmed, A. Azzeer, V. S. Yakovlev, V. Pervak, F. Krausz, and E. Goulielmakis, *Science* **334**, 195 (2011).
- [11] B. Alonso, M. Miranda, Í. J. Sola, and H. Crespo, *Opt. Express* **21**, 5582 (2013).
- [12] B. Alonso, Í. J. Sola, J. San Román, Ó. Varela, and L. Roso, *J. Opt. Soc. Am. B* **28**, 1807 (2011).
- [13] B. Alonso, M. Miranda, F. Silva, V. Pervak, J. Rauschenberger, J. San Román, Í. J. Sola, and H. Crespo, *Appl. Phys. B* **112**, 105 (2013).
- [14] B. Alonso, R. Borrego-Varillas, O. Mendoza-Yero, Í. J. Sola, J. San Román, G. Mínguez-Vega, and L. Roso, *J. Opt. Soc. Am. B* **29**, 1993 (2012).
- [15] G. Mínguez-Vega, C. Romero, O. Mendoza-Yero, J. V. de Aldana, R. Borrego-Varillas, C. Méndez, P. Andrés, J. Lancis, V. Climent, and L. Roso, *Opt. Lett.* **35**, 3694 (2010).
- [16] R. Borrego-Varillas, C. Romero, O. Mendoza-Yero, G. Mínguez-Vega, I. Gallardo, and J. V. de Aldana, *J. Opt. Soc. Am. B* **30**, 2059 (2013).
- [17] B. Alonso, R. Borrego-Varillas, Í. J. Sola, Ó. Varela, A. Villamarín, M. V. Collados, J. San Román, J. M. Bueno, and L. Roso, *Opt. Lett.* **36**, 3867 (2011).
- [18] E. J. Gualda, J. M. Bueno, and P. Artal, *J. of Biomedical Optics* **15**, 026007 (2010).
- [19] J. A. Wheeler, A. Borot, S. Monchocé, H. Vincenti, A. Ricci, A. Malvache, R. Lopez-Martens, and F. Quéré, *Nat. Photon.* **6**, 829 (2012).

- [20] C. Hernández-García, A. Jaron-Becker, D. D. Hickstein, A. Becker, and C. G. Durfee, *Phys. Rev. A* **93**, 023825 (2016).
- [21] W. Holgado, C. Hernández-García, B. Alonso, M. Miranda, F. Silva, L. Plaja, H. Crespo, and I. Sola, *Phys. Rev. A* **93**, 013816 (2016).
- [22] M. Miranda, C. L. Arnold, T. Fordell, F. Silva, B. Alonso, R. Weigand, A. L'Huillier, and H. Crespo, *Opt. Express* **20**, 18732 (2012).
- [23] M. Miranda, J. Penedones, C. Guo, A. Harth, M. Louisy, L. Neoričić, A. L'Huillier, and C. L. Arnold, *J. Opt. Soc. Am. B* **34**, 190 (2017).
- [24] J. Pérez-Hernández, L. Roso, and L. Plaja, *Laser Phys.* **19**, 1581 (2009).
- [25] C. Hernández-García, J. Pérez-Hernández, J. Ramos, E. Conejero Jarque, L. Roso, and L. Plaja, *Phys. Rev. A* **82**, 033432 (2010).
- [26] C. Hernández-García, T. Popmintchev, M. Murnane, H. Kapteyn, L. Plaja, A. Becker, and A. Jaron-Becker, *New J. of Phys.* **18**, 073031 (2016).
- [27] C. Hernández-García, W. Holgado, L. Plaja, B. Alonso, F. Silva, M. Miranda, H. Crespo, and I. Sola, *Opt. Express* **23**, 21497 (2015).
- [28] C. Hernández-García, I. Sola, and L. Plaja, *Phys. Rev. A* **88**, 043848 (2013).
- [29] M. Kretschmar, C. Hernández-García, D. S. Steingrube, L. Plaja, U. Morgner, and M. Kovačev, *Phys. Rev. A* **88**, 013805 (2013).
- [30] D. D. Hickstein, F. J. Dollar, P. Grychtol, J. L. Ellis, R. Knut, C. Hernández-García, D. Zusin, C. Gentry, J. M. Shaw, T. Fan, K. M. Dorney, A. Becker, A. J.-B. and Henry C. Kapteyn, M. M. Murnane, and C. G. Durfee, *Nat. Photon.* (2015).
- [31] C. Hernández-García, A. Picón, J. San Román, and L. Plaja, *Phys. Rev. Lett.* **111**, 083602 (2013).
- [32] E. Conejero Jarque, J. San Román, F. Silva, R. Romero, W. Holgado, M. A. González-Galicia, I. Sola, and H. Crespo, submitted (2017).
- [33] D. Fabris, W. Holgado, F. Silva, T. Witting, J. W. Tisch, and H. Crespo, *Opt. Express* **23**, 32803 (2015).
- [34] C. M. Heyl, H. Coudert-Alteirac, M. Miranda, M. Louisy, K. Kovacs, V. Tosa, E. Balogh, K. Varjú, A. L'Huillier, A. Couairon, and C. L. Arnold, *Optica* **3**, 75 (2016).
- [35] F. Böhle, M. Kretschmar, A. Jullien, M. Kovacs, M. Miranda, R. Romero, H. Crespo, U. Morgner, P. Simon, R. Lopez-Martens, and T. Nagy, *Laser Phys. Lett.* **11**, 095401 (2014).
- [36] H. Wang, Y. Wu, C. Li, H. Mashiko, S. Gilbertson, and Z. Chang, *Opt. Express* **16**, 14448 (2008).
- [37] P. Rudawski, A. Harth, C. Guo, E. Lorek, M. Miranda, C. M. Heyl, E. W. Larsen, J. Ahrens, O. Prochnow, T. Binhammer, U. Morgner, J. Mauritsson, A. L'Huillier, and C. L. Arnold, *The European Phys. J. D* **69**, 1 (2015).